Grooved Laminated Waveguide devices for U-, V-, W-and G-band applications

Camilla Kärnfelt, Pascal Coant, Maïna Sinou, Jean-Philippe Coupez, Daniel Bourreau, Alain Peden

Grooved Laminated Waveguide Devices for U-, V-, W- and G-band Applications

Camilla Kärnfelt, Pascal Coant, Maïna Sinou, Jean-Philippe Coupez, Daniel Bourreau and Alain Péden
Microwave Department, Télécom-Bretagne/Institut Mines Télécom
Lab-STICC UMR 6285
Brest, France
camilla.karnfelt@telecom-bretagne.eu

***Abstract*—This paper reports on the results of the design and manufacturing of straight sections, tees, bends and loads in a Grooved Laminated Waveguide (GLWG) topology. These devices, intended for the U-, V-, W- and G-band, are fabricated in Low Temperature Co-fired Ceramics (LTCC) technology using the low relative permittivity tape, ESL41110, from ElectroScience Laboratory. Measurements ranging from 40 to 170 GHz prove the concept of grooved laminated waveguides.**

***Keywords*—Grooved Laminated Waveguides; GLWG; LTCC; bend; tee; load; LWG; Millimeter wave devices**

I. Introduction

The Laminated Waveguide (LWG), which is a waveguide integrated in a multilayer dielectric substrate, was first patented in 1992 followed by a scientific publication in 1998, [1]. It has earned lots of attention recently in its one-layer form referred to as Substrate Integrated Waveguide (SIW). As a transmission support, the LWG/SIW has several advantages compared to other transmission line types such as the microstrip line or the stripline; it suffers less from losses and has a better isolation between adjacent lines. Also, due to its confinement, it is well suited for multilayer applications where different LWGs can be placed in separate layers, crossing each other, without any particular precautions to be taken.

One of the drawbacks of the LWG/SIW in their present form is the implementation of rows of metallized vias to form the vertical walls of the waveguide. The diameter and via-to-via distance have to be kept small to ensure minimal radiation. Design guide lines, e.g. in [2], proposes that the via diameter, d, should be less than $\lambda_g/5$, where λ_g is the guided wavelength, and the vias' center-to-center distance, p, should be less or equal to twice the via diameter. The requirement of a center-to-center distance less than two via diameters is often not supported from the fabrication point of view, but even when possible, these design guide lines indicates the frequency limits in the following way: using $p \leq 2 \times d$, $d \leq \lambda_g/5$, $\lambda_g = \lambda/\sqrt{(1-(f_c/f)^2)}$ and $\lambda = c_0/(f \times \sqrt{\varepsilon_r})$ where f_c denotes the cut off frequency, c_0 the speed of light and ε_r the relative permittivity, and taking λ_g at f equals $1.9 \times f_c$, i.e. at the upper end of the waveguide band, we obtain (1) as an expression of maximum frequency related to the center-to-center distance and the relative permittivity.

$$f_{max} \leq \frac{2c_0 \times 1.176}{5p\sqrt{\varepsilon_r}} \quad (1)$$

From this relation it is quite obvious that a lower relative permittivity is advantageous for higher frequency as is, off course, a smaller via pitch. At a certain point, a good trade-off between fabrication ease and radiation minimization can no longer be achieved, which leads to that the metallized via rows should be avoided in the upper millimeter-wave region.

With the objective to develop a packaging concept for devices up to at least G-band, this is the main argument to why we considered using Grooved Laminated Waveguides (GLWG) instead. This topology, where the two via rows are replaced by metallized grooves along the whole waveguide structure, was studied in [3], however, only straight sections were realized. In this work, other elements with more challenging geometries were manufactured to prove the feasibility of the GLWG topology.

II. Material Choice and Data

Low Temperature Co-fired Ceramics (LTCC) is an excellent choice for implementation of GLWGs as was already proven using in 254 µm thick DuPont943PX tape, [3]. LTCC is a true multilayer technology with a Coefficient of Thermal Expansion (CTE) close to that of GaAs, GaN and Si used for MMIC components (Microwave Monolithic Integrated Circuit). As compared to other suppliers, ElectroScience Laboratory offers quite a vast choice of different LTCC tapes, [4], with low, medium and high relative permittivities which is valuable in the scope of designing devices for a large range of frequencies keeping a small form factor.

In our case, we have opted for the ESL41110 tape which, with its low relative permittivity ($\varepsilon_r \approx 4.4$, $\tan\delta \approx 0.009$ at 10 GHz) relaxes the manufacturing constraints when increasing the frequency towards the mm-wave range.

III. Fabrication Process

The ESL41110 tape is delivered in a rolled sheet of about 100 µm thickness. After sintering, the sheet thickness is 75-80 µm. ESL803 gold paste is used for the conductors (top and bottom metal plates of the GLWGs) and the grooves are filled using the ESL802 gold paste intended for metallizing via holes.

Our manufacturing process follows the standard procedure proposed by ESL; blanking, laser cutting, screen printing (via and groove filling and conductor printing), stacking, lamination and co-firing. To manufacture these GLWG structures, some non-mainstream process steps have been added such as groove cutting and filling, a second laser cutting operation is introduced between the screen printing and the stacking step, a cavity filling step is added after sintering and finally a laser ablation step is done after co-firing. Details on the manufacturing issues can be found in [5]. Fig. 1 shows the two substrates of this work in different production stages.

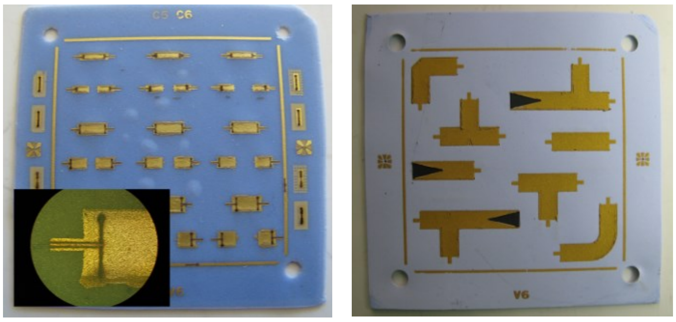

Fig. 1. The two prototype substrates. Left; The first row from the top includes the G-band GLWGs, the third row, the W-band version and the fifth row the V-band version. The inset shows a micrograph detailing the laser ablation. Right; Substrate containing U-band devices (all realized as one layered GLWGs) here seen after lamination. The black inserts are the fugitive tape that burn out during the sintering step to leave room for an absorbent material.

IV. GLWG Devices: Design and Measurement

A. Coplanar to waveguide transition

In order to measure the proposed GLWG devices in a probe-station, a CPW to GLWG transition, as suggested in [6], was used. For the V-, W- and G-band devices we opted for a 100 µm pitch ground-signal-ground (GSG) probe from Picoprobe. For the U-band devices, a 150 µm pitched probe from the same company was used and the CPW lines were designed accordingly. In both cases the length of the CPW line is set to 1 mm. The transitions were adjusted for each type of GLWG band. The transitions' in-band simulated insertion loss is given in TABLE I. , according to results from full 3D simulations using CST Microwave Studio. However, in the region below 1.25 × f_c, a transmission dip is always present due to a standing wave that appears from the transversal slots. Fig. 3 gives the dimensions for one of the devices, including the transition.

B. Lines

One-layer GLWG straight sections were designed and measured for the four bands U, V, W and G. The W- and G-lines were also fabricated using four LTCC layers where the grooves were then placed in the four top layers of the LTCC stack, Fig. 4. (Only the G-band four layered GLWG was successful).

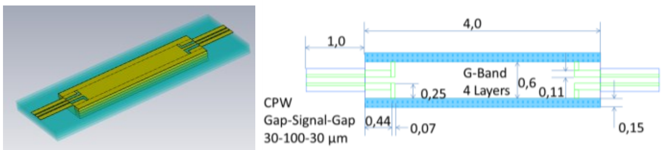

Fig. 2. GLWG sections. Left; Four-layered GLWG with CPW to GLWG transitions. The translucide blue is LTCC and the yellow parts are gold. This structure is placed on top of several empty LTCC layers in order to rigidify the device. Right: Dimensions of the G-band four-layered GLWG section. All measures in mm unless otherwise stated. The total length including 2×1mm CPW-lines is 10.5 mm for the U-band and 6 mm for the V-, W-, and G-band devices.

These samples are fabricated with the intention to study if such GLWGs are possible to manufacture in a convenient way. Design and simulation data is given in TABLE I.

TABLE I. GLWG design data

Device characteristics	Band				
	U	***V***	***W***	***G***	
Number of layers[a] [µm]	1	1	1	1	4
Inner width a [µm]	2250	1770	1200	600	
GLWG section length (without transition) [mm]	7.3	2.8	2.8	2.8	
α_{line}[b] [dB/mm]	0.1	0.125	0.185	0.40	

a. Each layer is 75 µm, thus the b dimension equals the number of layers multiplied by 75 µm

b. Simulated data for a GLWG line (without transition) in the center band, εr=4.5 and tanδ=0.008

One of the G-band GLWGs were cut through in order to measure the dimension *a*, i.e. the inner width, of the GLWG. More cross sections should be done to confirm the dimensions.

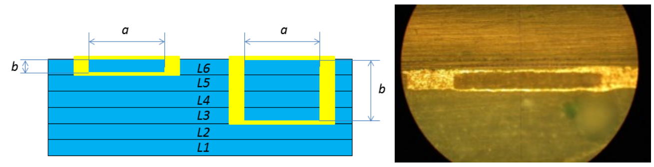

Fig. 3. Left: Layer stack for one and four-layered GLWG having an inner height of 75 and 300 µm respectively Right: Micrograph of cross-section of one of the one-layered G-band GLWGs. The inner dimension is found to be 610 × 75 µm at the position of the cut. The gold filled grooves are 180 µm wide. Measurement tolerance is ± 5 µm. LTCC is filling the portion below the GLWG in the micrograph.

Simulation and measurement data are given in Fig. 4 for the four bands. (Throughout this document, data from retro-simulation, corrected for dimensional errors, is used together with ε_r=4.5 and tanδ=0.008). The U-band straight section performs quite well, but has some additional losses in the lower frequency band.

The V-band transition has a large dip from 42 to 50 GHz in its transmission loss curve, which is also shifted about 1 GHz upwards in frequency. The other GLWG-sections exhibit the same kind of dip but less pronounced, thus, the V-band transition could have been optimized for better performance.

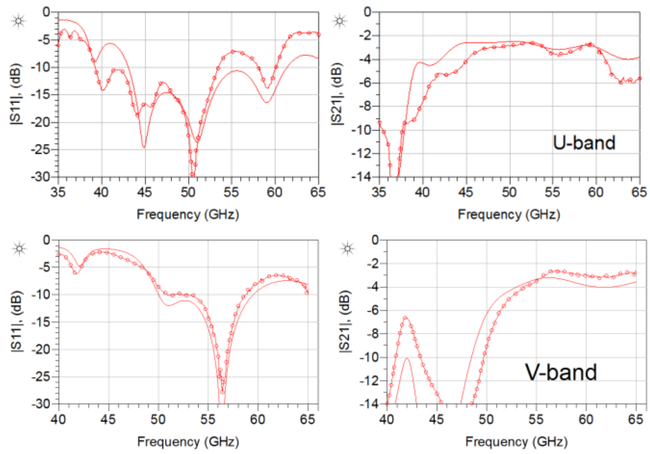

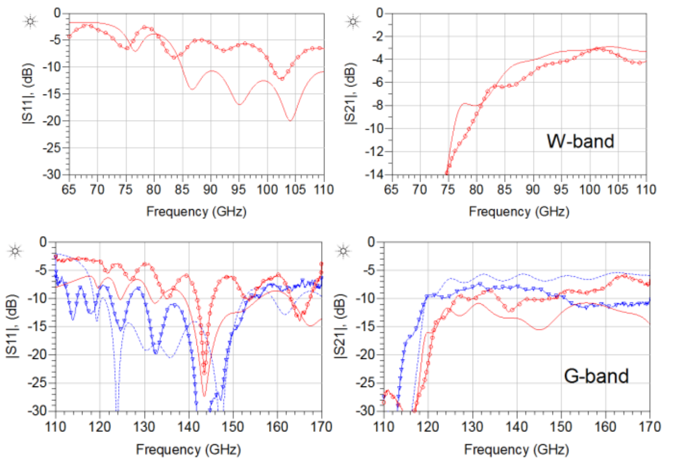

Fig. 4. Retro-simulated (one-layer: red line, four-layers: blue dashed line) and measured (one-layer: red circles, four-layers: blue triangles) results for the GLWG straight sections.

The G-band and W-band one-layer sections have a reflection coefficient less good than expected, which affects the performance in a negative manner. This seems to be due to a non-50 Ω impedance seen at the probe position of the CPW lines. The four layered G-band section has somewhat lesser losses than the one-layered version up to 150 GHz, but comprises more losses at the higher frequency end. Thus it is hard to conclude on the benefits of a multi-layer GLWG.

Globally the measured data follows the simulated results quite well when adjusting for dimensional data and taking into account the ablation depth (which was not considered initially). Still, after correction, some difference persists which may be caused by a non-correct relative permittivity over some of (or the whole) frequency range, dimensional variations, or attributable to the roughness on the inside of the grooves.

C. Load

A termination load is a useful device and some publications have been presented on the subject of SIW loads for the X-band. In [7] a thin film resistor (TFR) was placed at the end of a short circuited SIW. A rectangular and two tapered shapes were tested with an acceptable return loss. The better solution was found to be the longer tapered TFR. In [8] an insert of an absorbing material was placed either as a rectangular shape (narrow band solution) at the end of the short circuited SIW or as a taper long one of the via walls (wide band solution). In this work, we have tried a solution based on a centered taper-shaped absorber; the top metal and the dielectric material of the GLWG are opened in a triangular form and the cavity is filled with an absorbing material. The further end of the GLWG is not short-circuited. In simulation we have used different resistive pastes, normally intended for screen printing thick film resistors with the best result achieved when using 1000 Ω/□. The longer the taper length the better, we finally decided on a taper length twice the width of the GLWG.

The load is realized as a stand-alone device for validation and as a termination load integrated with port 2 on two types of tees. In measurement, Fig. 5, we have compared the 1000 Ω/□ paste with the Eccosorb MMI-SA. Their performance is about the same and unfortunately not as good as expected, probably due to insufficient absorption of the absorbent material over the frequency range, thus a portion of the incoming signal is reflected.

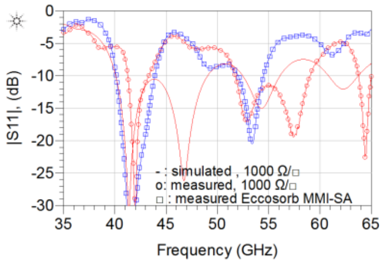

Fig. 5. Retro-simulated and measured results (all including the CPW to GLWG transition) from of the U-band loads.

D. Bends

From the LWG/SIW publications, few analyses on bends are published. However, thorough studies have been made earlier on regular rectangular hollow waveguides. In [9], different types of H-plane bends are analyzed, such as un-mitered bends, fully mitered bends and mitered bends with different *t/a* ratios. In that work, optimal performance of the bend was found with a *t/a* ratio of 0.386. About the same result was found in [10] where the *c/a* ratio of 0.63 (i.e. *t/a* ratio of 0.37) was found to be the best. For both these publications the studied waveguides were of rectangular hollow metal type, with the height close to half the width (however not explicitly stated).

In our case two types of U-band H-plane 90° bends were designed; one curved with a large radius and one with a 45° miter at the outer corner having a right angled inner bend where the (non-optimized) *t/a* ratio is 0.43, which should account for a quite good performance. Fig. 6 gives the dimensions.

Fig. 7 shows the simulated (without and with the transition) and measured (including transitions) S-parameters for these two bends. From simulation without the transitions, the curved bend has a better reflection coefficient, suffers from somewhat higher losses due to the longer path but performs better at the high end of the frequency band. With the transitions included the two bends are rather equal in performance. In measurement, the curved bend is somewhat better at lower frequencies.

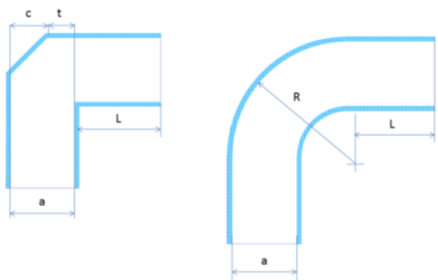

Fig. 6. U-band bend dimensions; *a*=2250 µm, *t*=965 µm, *c*= 1285 µm, *L*= 2850 µm and, *R*= 4000 µm. The waveguide inner height is 75 µm. For a just comparison dimensions *a* and *L* are kept the same between the two bends. The grooves are 150 µm wide. Left; mitered bend, Right; curved bend.

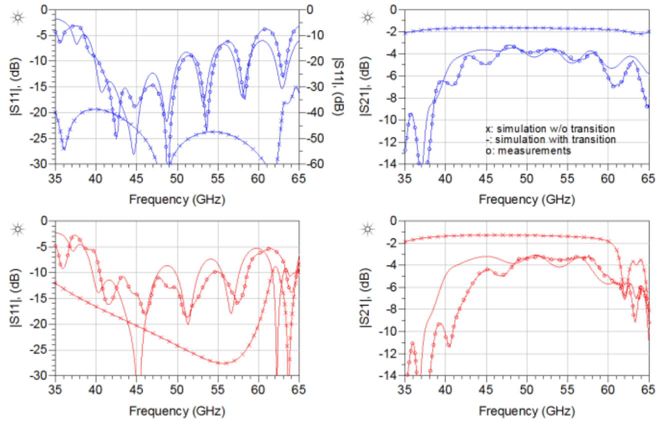

Fig. 7. Comparison of retro-simulated and measured data of the bends; blue curves denotes the curved bend and red curves denote the mitered bend.

E. Tees

Symmetric tees dividing the signal in equal phase and equal amplitude were also realized. Two solutions were implemented; one using a metallized via to control the power split ratio (to be 1:1 in this case) and to improve the input matching. In the second design, a groove peak was used to do the same job. The designs' dimensions (without the transitions) are given in Fig. 8 and the S-parameters are given in Fig. 9.

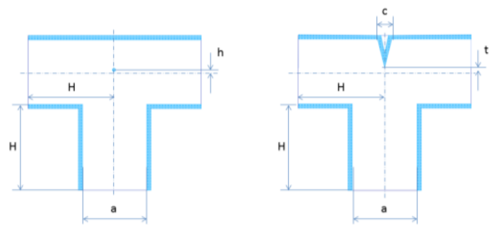

Fig. 8. U-band tee dimensions; a=2250µm, H=3000 µm, h=75 µm, t=135 µm and c=500 µm. The waveguides' inner height is 75 µm. Left; the tee with the via, Right; tee with peaked groove.

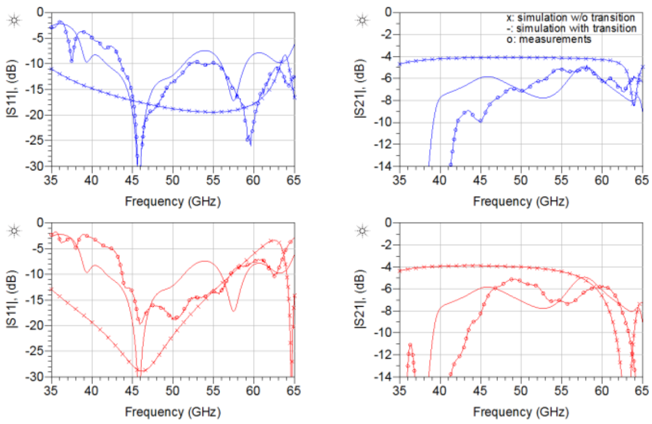

Fig. 9. Comparison between retro-simulated and measured data for two U-band tees: blue curves denote the grooved peak tee, red curves denote the tee with via. The third acces is terminated by a 50 Ω external load connected to the probe in the probe station.

From Fig. 9, comparing the data for the tees without transitions, it seems that the peaked tee design has a better wide band behavior, as compared to the tee with a single via inserted in the junction. The tee with the via is evidently not optimized at the U-band central frequency, i.e. 50 GHz, but at 46 GHz, so its performance could be somewhat improved in a future run. However, even when optimizing (h=200 µm) the band width is less large than for the grooved peak tee. The measurement data follows the retro-simulated data quite well, but we have a frequency shift of about 2 GHz. The tees with an absorbent load connected to the third access, seen on the right photo of Fig. 1, performed badly why no measured data is presented.

Conclusions

Different U-, V-, W- and G-band devices were successfully realized in GLWG topology using a low relative permittivity LTCC. One- and four-layered GLWG lines were realized and compared at G-band. In the U-band, more complex geometries such as bends, tees and loads were successfully achieved. The results prove the feasibility of GLWG grooved LTCC devices up to at least 170 GHz with possibility to reach even higher.

Acknowledgment

The authors would like to thank the last year students Lamyae Khibabi and Benoît Fauré for their work on the bends and tees, and Ph.D. Khodor Rida for his efforts to set up the LTCC platform. Also thanks to Mr. Michel Bilinski from ESL for good advice throughout this work and to the scientific direction and Microwave department of Télécom-Bretagne for their funding.

References

[1] H. Uchimura, T. Takenoshita, and M. Fujii, "Development of a laminated waveguide," *IEEE Transactions on Microwave Theory and Techniques*, vol. 46, n° 12, pp. 2438‑2443, dec. 1998.

[2] T. Djerafi and K. Wu, "Substrate Integrated Waveguide (SIW) Techniques: The State-f-the-Art Developments and Future Trends," *Journal of University of Electronic Science of China*, vol. 42, n° 2, pp. 171‑192, mars 2013.

[3] M. F. Shafique and I. D. Robertson, "Laser machining of microvias and trenches for substrate integrated waveguides in LTCC technology," in *Microwave Conference, 2009. EuMC 2009. European*, 2009, pp. 272–275.

[4] "ESL ElectroScience Products - Ceramic Green Tapes". [On line]. Available at: http://www.electroscience.com/ceramictapes.html. [Consulted on: 12-may-2015].

[5] C. Kärnfelt, P. Coant, M. Sinou, J.-P. Coupez, D. Bourreau, and A. Péden, "Grooved Laminated Waveguides in LTCC for mm-wave packaging," Micro/Nano-electronics Packaging and Assembly, Design and manufacturing Forum, (MiNaPAD2015), Grenoble, 2015.

[6] D. Deslandes and K. Wu, "Integrated transition of coplanar to rectangular waveguides," in *Microwave Symposium Digest, 2001 IEEE MTT-S International*, 2001, vol. 2, pp. 619‑622 vol.2.

[7] H. Uchida, M. Nakayama, A. Inoue, and Y. Hirano, "A Post-Wall Waveguide (SIW) Matched Load with Thin-Film Resistor," in *Proceedings*, 2010, pp. 1597‑1600.

[8] H. Chen, W. Che, Q. Li, C. Gu, and K. Wu, "Substrate-integrated waveguide matching terminations with microwave absorbing material," *Electronics Letters*, vol. 50, n° 17, pp. 1216‑1218, aug. 2014.

[9] F. Alimenti, M. Mongiardo, and R. Sorrentino, "Design of mitered H-plane bends in rectangular waveguides by combined mode matching and finite differences," IEEE Microwave Conference, 1994. 24th European, 1994, vol. 1, pp. 289‑293.

[10] Z. Ma, T. Yamane, and E. Yamashita, "Analysis and design of H-plane waveguide bends with compact size, wide-band and low return loss characteristics," in *IEEE MTT-S International Microwave Symposium Digest*, 1997, vol. 2, pp. 417‑420.